RESEARCH ARTICLE

NUMERICAL SOLUTIONS OF REACTION-DIFFUSION EQUATION SYSTEMS WITH TRIGONOMETRIC QUINTIC B-SPLINE COLLOCATION ALGORITHM

Aysun TOK ONARCAN [1] , **Nihat ADAR** [2] , **Idiris DAG** [2]

[1] Department of Informatics, Eskişehir Osmangazi University, Eskişehir, Türkiye
[2] Department of Computer Engineering, Eskişehir Osmangazi University, Eskişehir, Türkiye

ABSTRACT

In this study, trigonometric quintic B-spline collocation method is constructed for computing numerical solutions of the reaction-diffusion system (RDS). Schnakenberg, Gray-Scott and Brusselator models are special cases of reaction-diffusion systems considered as examples in this paper. Crank-Nicolson formulae is used for the time discretization of the generalized RDS and the nonlinear terms in time-discretized form of RDS are linearized using the Taylor expansion. The fully integration of the generalized system is carried out using the collocation method based on the trigonometric quintic B-splines. The method is tested on different problems to illustrate the accuracy. The error norms are calculated for the linear problem whereas the relative error is given for nonlinear problems. Both simple and easy B-spline algorithms are illustrated to give the solutions of RDS and also the graphical representation of the efficient solutions are presented for the nonlinear RDSs. Combination of the quintic B-splines and the collocation method is shown to present numerical solutions of the RDS successfully. With the presented method, it is possible to get approximate solutions as well as their derivatives up to an order of four on the problem domain.

Keywords: Reaction-diffusion; Collocation; B-spline; Finite element method, Brusselator, Schnakenberg, Gray-Scott

1. INTRODUCTION

In various disciplines, phenomena such as pattern formation, autocatalytic chemical reactions and population dynamics are modelled by the reaction-diffusion (RD) equation systems. These RDSs are mathematical models of chemical exchange reactions some of which of them also generates various patterns in biology, geology, physics and ecology. RDSs exhibit very rich dynamics behavior including periodic and quasi-periodic solutions. Theoretical studies have been developed to describe such dynamic behaviors. Most diffusion systems include the nonlinear reaction term making it difficult to solve analytically. Attempts have been made to look for the numerical solutions to reveal more dynamic behaviors of RDSs. Various numerical methods also have been used to find the numerical solutions of RDSs.

In the past, implicit-explicit method was designed to obtain some type of patterns, as a solution of RD equations by Ruuth [1]. An adaptive moving mesh method and a moving grid finite element method were produced for the numerical solutions of RDS respectively [2, 3]. Operator splitting methods were set up to solve RDSs in the studies [4, 5]. Both a Crank-Nicholson method with a Multi-Grid solver (CN-MG) and the implicit integration factor method were presented in the study [6]. Galerkin finite element method was constructed for getting numerical solutions of the RDSs [7]. Additionally, the differential quadrature (DQ) method was constructed for calculating numerical solutions of RDSs by Mittal et all. [8] and Jiwari et all. [9]. Recently, Jiwari presented a kind of DQ method for capturing various patterns [10].

The spline functions of various degrees are accompanied to construct numerical methods for solving differential equations of certain order. Since the resulting matrix obtained for application of the spline related numerical method to the differential equation is always diagonal, it can be solved easily. High order continuous differentiable approximate solutions can be produced by way of using high order spline functions for solutions of the differential equations. B-splines are defined as a basis of the spline space[11]. Polynomial B-splines are extensively used for finding numerical solutions of differential equations, function approximation and computer-aided design. The numerical procedure based on the B-spline collocation method has been increasingly applied for nonlinear evolution equations in various fields of science [12]-[16]. The numerical methods for solving types of ordinary differential equations with trigonometric quadratic and cubic B-spline were given by A. Nikolis [17, 18]. Numerical solutions of RD systems with polynomial B-spline collocation method (PQBCM) was presented in the work of Sahin [19]. Exponential cubic B-spline algorithm for the system of RD equations was presented by Ersoy O. and Dag I.[20] and trigonometric cubic B-spline algorithm was studied by Onarcan et all [21]. Specific RDS models were studied with finite element methods by the researchers [22, 23]. Very recently Hepson O.E. and others applied quartic trigonometric tension B-spline collocation method to get some numerical simulations of RDS [24].

In this study, we use the fifth degree trigonometric B-spline termed as trigonometric quintic B-spline (TQB) to establish a collocation method to find numerical solutions of a reaction-diffusion equation systems. In the literature review, it has been found that few studies have been done with trigonometric quintic of B-spline [25]-[28]. With the TQB based collocation method that we presented, it is possible to get approximate solutions as well as its derivatives up to an order of four at each point of the problem domain. Linear problem and nonlinear Brusselator [29], Schnakenberg [30] and Gray-Scott [31] models are studied with the proposed TQB collocation method.

One dimensional time-dependent reaction-diffusion equation systems can be defined as follows:

$$\frac{\partial U}{\partial t} = D_u \frac{\partial^2 U}{\partial x^2} + F(U, V)$$

$$\frac{\partial V}{\partial t} = D_v \frac{\partial^2 V}{\partial x^2} + G(U, V) \tag{1}$$

where $U = U(x, t), V = V(x, t)$ and $\Omega \subset R^2$ is the problem domain, D_u is the diffusion coefficient of U and D_v is the diffusion coefficients of V also F and G indicates the growth and interaction functions that represent the reactions of the system. F and G are, in general, nonlinear functions. A general one dimensional RD equation system which includes all test problems mentioned in this paper, is expressed as:

$$\frac{\partial U}{\partial t} = a_1 \frac{\partial^2 U}{\partial x^2} + b_1 U + c_1 V + d_1 U^2 V + e_1 UV + m_1 UV^2 + n_1$$

$$\frac{\partial V}{\partial t} = a_2 \frac{\partial^2 V}{\partial x^2} + b_2 U + c_2 V + d_2 U^2 V + e_2 UV + m_2 UV^2 + n_2 \tag{2}$$

For computational purpose, solution space of the problems $(-\infty, \infty)$ should be limited to interval (x_0, x_N). In this case, system (2)'s initial conditions are either the homogenous boundary conditions of Dirichlet

$$U(x_0, t) = U(x_N, t) = 0, \qquad V(x_0, t) = V(x_N, t) = 0, \tag{3}$$

or homogeneous Neumann boundary conditions

$$U_x(x_0, t) = U_x(x_N, t) = 0, \qquad V_x(x_0, t) = V_x(x_N, t) = 0 \tag{4}$$

The coefficients of the system (2) are depicted in Table 1, matching the coefficients of the test problems appropriately according to the characteristics of each test problem.

Table 1: Matching the coefficients of test problems with the model system

Test Problem	a_1	a_2	b_1	b_2	c_1	c_2	d_1	d_2	e_1	e_2	m_1	m_2	n_1	n_2
Linear	d	d	$-a$	0	1	$-b$	0	0	0	0	0	0	0	0
Brusselator	ε_1	ε_2	$-(B+1)$	B	0	0	1	-1	0	0	0	0	A	0
Schnakenberg	1	d	$-\zeta$	0	0	0	ζ	$-\zeta$	0	0	0	0	ζa	ζb
Gray-Scott	ε_1	ε_2	$-f$	0	0	$-k$	0	0	0	0	-1	1	f	0

2. TRIGONOMETRIC QUINTIC B-SPLINE METHOD

Consider the solution domain of the differential problem $[a = x_0, b = x_N]$ is partitioned into a mesh of uniform length $h = x_{m+1} - x_m$ by knots x_m, where $m = -2, \dots, N + 2$. On this partition, together with additional knots $x_{N-2}, x_{N-1}, x_{N+1}, x_{N+2}$ outside the problem domain, the trigonometric quintic B-spline $T_m^5(x)$ basis functions at knots are given as:

$$T_m^5(x) = \frac{1}{\theta} \begin{cases} \rho^5(x_{m-3}), & x \in [x_{m-3}, x_{m-2}] \\ -\rho^4(x_{m-3})\rho(x_{m-1}) - \rho^3(x_{m-3})\rho(x_m)\rho(x_{m-3}) \\ -\rho^2(x_{m-3})\rho(x_{m+1})\rho^2(x_{m-2}) - \rho(x_{m-3})\rho(x_{m+2})\rho^3(x_{m-2}) \\ -\rho(x_{m+3})\rho^4(x_{m-2}), & x \in [x_{m-2}, x_{m-1}] \\ \rho^3(x_{m-3})\rho^2(x_m) + \rho^2(x_{m-3})\rho(x_{m+1})\rho(x_{m-2})\rho(x_m) \\ +\rho^2(x_{m-3})\rho^2(x_{m+1})\rho(x_{m-1}) + \rho(x_{m+3})\rho(x_{m+2})\rho^2(x_{m-2})\rho(x_m) \\ +\rho(x_{m-3})\rho(x_{m+2})\rho(x_{m-2})\rho(x_{m+1})\rho(x_{m-1}) + \rho(x_{m-3})\rho^2(x_{m+2})\rho^2(x_{m-1}) \\ +\rho(x_{m+3})\rho^3(x_{m-2})\rho(x_m) + \rho(x_{m+3})\rho^2(x_{m-2})\rho(x_{m+1})\rho(x_{m-1}) \\ +\rho(x_{m+3})\rho(x_{m-2})\rho(x_{m+2})\rho^2(x_{m-1}) + \rho^2(x_{m+3})\rho^3(x_{m-1}), & x \in [x_{m-1}, x_m] \\ -\rho^2(x_{m-3})\rho^3(x_{m+1}) - \rho(x_{m-3})\rho(x_{m+2})\rho(x_{m-2})\rho^2(x_{m+1}) \\ -\rho(x_{m-3})\rho^2(x_{m+2})\rho(x_{m-1})\rho(x_{m+1}) - \rho(x_{m-3})\rho^3(x_{m+2})\rho(x_m) \\ -\rho(x_{m+3})\rho^2(x_{m-2})\rho^2(x_m) - \rho(x_{m+3})\rho(x_{m-2})\rho(x_{m+2})\rho(x_{m-1})\rho(x_{m+1}) \\ -\rho(x_{m+3})\rho(x_{m-2})\rho^2(x_{m+2})\rho(x_m) - \rho^2(x_{m+3})\rho^2(x_{m-3}) \\ -\rho^2(x_{m+3})\rho(x_{m-1})\rho(x_{m+2})\rho(x_m) - \rho^3(x_{m+3})\rho^2(x_m), & x \in [x_m, x_{m+1}] \\ \rho(x_{m-3})\rho^4(x_{m+2}) \\ +\rho(x_{m+3})\rho(x_{m-2})\rho^3(x_{m+2}) + \rho^2(x_{m+3})\rho(x_{m-1})\rho^2(x_{m+2}) \\ +\rho^3(x_{m+3})\rho(x_m)\rho(x_{m+2}) + \rho^4(x_{m+3})\rho(x_{m+1}), & x \in [x_{m+1}, x_{m+2}] \\ -\rho^5(x_{m+3}), & x \in [x_{m+2}, x_{m+3}] \\ 0, & \text{otherwise} \end{cases} \tag{5}$$

where $\rho(x_m)$, θ and m are;

$$\rho(x_m) = sin(\frac{x - x_m}{2}),$$

$$\theta = sin(\frac{5h}{2})sin(2h)sin(\frac{3h}{2})sin(h)sin(\frac{h}{2}),$$

$$m = 0(1)N.$$

The $T_m^5(x)$ functions and its principle derivatives vanish outside the region $[x_{m-3}, x_{m+3}]$. The set of those B-splines $T_m^5(x)$, $m = -2, \ldots, N + 2$ are a basis for the trigonometric spline space. An approximate solution $U_N(x, t)$ and $V_N(x, t)$ to the unknown solution $U(x, t)$ and $V(x, t)$ can be assumed as the forms

$$U_N(x, t) = \sum_{i=-2}^{N+2} T_i^5(x)\delta_i(t), \quad V_N(x, t) = \sum_{i=-2}^{N+2} T_i^5(x)\gamma_i(t) \tag{6}$$

Where δ_i and γ_i are time dependent parameters to be determined using the collocation method on the points x_i, $i = 0, \ldots, N$ together with boundary and initial conditions. $T_m^5(x)$ trigonometric quintic B-spline functions are zero outside the interval $[x_{m-3}, x_{m+3}]$ and $T_m^5(x)$ functions sequentially covers six elements in the interval $[x_{m-3}, x_{m+3}]$ so that, each $[x_m, x_{m+1}]$ finite element is covered by the six $T_{m-2}^5, T_{m-1}^5, T_m^5, T_{m+1}^5, T_{m+2}^5$, and T_{m+3}^5 trigonometric quintic B-spline. In this case the approach (6) can be written as ;

$$U_N(x, t) = \sum_{i=m-2}^{m+3} T_i^5(x)\delta_i = T_{m-2}^5(x)\delta_{m-2} + T_{m-1}^5(x)\delta_{m-1} + T_m^5(x)\delta_m + T_{m+1}^5(x)\delta_{m+1}$$
$$+ T_{m+2}^5(x)\delta_{m+2} + T_{m+3}^5(x)\delta_{m+3}$$

$$V_N(x, t) = \sum_{i=m-2}^{m+3} T_i^5(x)\gamma_i = T_{m-2}^5(x)\gamma_{m-2} + T_{m-1}^5(x)\gamma_{m-1} + T_m^5(x)\gamma_m + T_{m+1}^5(x)\gamma_{m+1}$$
$$+ T_{m+2}^5(x)\gamma_{m+2} + T_{m+3}^5(x)\gamma_{m+3} \tag{7}$$

In these numerical approaches, the approximate solutions and its first, second, third and fourth derivative at the knots can be written in terms of the time parameters using $T_m^5(x)$ and Eq.(6) as given in the following relationships:

$$U_m = \alpha_1\delta_{m-2} + \alpha_2\delta_{m-1} + \alpha_3\delta_m + \alpha_2\delta_{m+1} + \alpha_1\delta_{m+2}$$
$$U_m' = -\alpha_4\delta_{m-2} - \alpha_5\delta_{m-1} + \alpha_5\delta_{m+1} - \alpha_4\delta_{m+2}$$
$$U_m'' = \alpha_6\delta_{m-2} + \alpha_7\delta_{m-1} + \alpha_8\delta_m + \alpha_7\delta_{m+1} + \alpha_6\delta_{m+2}$$
$$U_m''' = -\alpha_9\delta_{m-2} + \alpha_{10}\delta_{m-1} - \alpha_{10}\delta_{m+1} - \alpha_9\delta_{m+2}$$
$$U_m'''' = \alpha_{11}\delta_{m-2} + \alpha_{12}\delta_{m-1} + \alpha_{13}\delta_m + \alpha_{12}\delta_{m+1} + \alpha_{11}\delta_{m+2} \tag{8}$$
$$V_m = \alpha_1\gamma_{m-2} + \alpha_2\gamma_{m-1} + \alpha_3\gamma_m + \alpha_2\gamma_{m+1} + \alpha_1\gamma_{m+2}$$
$$V_m' = -\alpha_4\gamma_{m-2} - \alpha_5\gamma_{m-1} + \alpha_5\gamma_{m+1} + \alpha_4\gamma_{m+2}$$
$$V_m'' = \alpha_6\gamma_{m-2} + \alpha_7\gamma_{m-1} + \alpha_8\gamma_m + \alpha_7\gamma_{m+1} + \alpha_6\gamma_{m+2}$$
$$V_m''' = -\alpha_9\gamma_{m-2} + \alpha_{10}\gamma_{m-1} - \alpha_{10}\gamma_{m+1} + \alpha_9\gamma_{m+2}$$
$$V_m'''' = \alpha_{11}\gamma_{m-2} + \alpha_{12}\gamma_{m-1} + \alpha_{13}\gamma_m + \alpha_{12}\gamma_{m+1} + \alpha_{11}\gamma_{m+2}$$

where the coefficients are:

$$\alpha_1 = \frac{\sin^5(\frac{h}{2})}{\theta}$$

$$\alpha_2 = \frac{2\sin^5(\frac{h}{2})\cos(\frac{h}{2})(16\cos^2(\frac{h}{2}) - 3)}{\theta}$$

$$\alpha_3 = \frac{2(1 + 48\cos^4(\frac{h}{2}) - 16\cos^2(\frac{h}{2})\sin^5(\frac{h}{2}))}{\theta}$$

$$\alpha_4 = \frac{\frac{5}{2}\sin^4(\frac{h}{2})\cos(\frac{h}{2})}{\theta}$$

$$\alpha_5 = \frac{5\sin^4(\frac{h}{2})\cos^2(\frac{h}{2})(8\cos^2(\frac{h}{2}) - 3)}{\theta}$$

$$\alpha_6 = \frac{\frac{5}{4}\sin^3(\frac{h}{2})(5\cos^2(\frac{h}{2}) - 1)}{\theta}$$

$$\alpha_7 = \frac{\frac{5}{2}\sin^3(\frac{h}{2})(\cos(\frac{h}{2})(-15\cos^2(\frac{h}{2}) + 3 + 16\cos^4(\frac{h}{2})))}{\theta}$$

$$\alpha_8 = \frac{-\frac{5}{2}\sin^3(\frac{h}{2})(16\cos^6(\frac{h}{2}) - 5\cos^6(\frac{h}{2}) + 1)}{\theta}$$

$$\alpha_9 = \frac{\frac{5}{8}\sin^2(\frac{h}{2})\cos(\frac{h}{2})(25\cos^2(\frac{h}{2}) - 13)}{\theta}$$

$$\alpha_{10} = \frac{-\frac{5}{4}\sin^2(\frac{h}{2})(\cos^2(\frac{h}{2})(8\cos^4(\frac{h}{2}) - 35\cos^2(\frac{h}{2}) + 15)}{\theta}$$

$$\alpha_{11} = \frac{\frac{5}{16}(125\cos^4(\frac{h}{2}) - 114\cos^2(\frac{h}{2}) + 13)\sin(\frac{h}{2}))}{\theta}$$

$$\alpha_{12} = \frac{-\frac{5}{8}\sin(\frac{h}{2})\cos(\frac{h}{2})(176\cos^6(\frac{h}{2}) - 137\cos^4(\frac{h}{2}) - 6\cos^2(\frac{h}{2}) + 15)}{\theta}$$

$$\alpha_{13} = \frac{\frac{5}{8}(92\cos^6(\frac{h}{2}) - 117\cos^4(\frac{h}{2}) + 62\cos^2(\frac{h}{2}) - 13)(-1 + 4\cos^2(\frac{h}{2})\sin(\frac{h}{2}))}{\theta}$$

(9)

The Crank–Nicholson formulas are used for time discretization.

$$U_t = \frac{U^{n+1} - U^n}{\Delta t}, \quad U = \frac{U^{n+1} + U^n}{2}, \quad V_t = \frac{V^{n+1} - V^n}{\Delta t}, \quad V = \frac{V^{n+1} + V^n}{2} \quad (10)$$

The unknown U and V functions and their derivatives are discretized to yield time integrated reaction-diffusion system:

$$\frac{U^{n+1} - U^n}{\Delta t} - a_1 \frac{U_{xx}^{n+1} + U_{xx}^n}{2} - b_1 \frac{U^{n+1} + U^n}{2} - c_1 \frac{V^{n+1} + V^n}{2} - d_1 \frac{(U^2V)^{n+1} + (U^2V)^n}{2}$$
$$- e_1 \frac{(UV)^{n+1} + (UV)^n}{2} - m_1 \frac{(UV^2)^{n+1} + (UV^2)^n}{2} - n_1 = 0$$

$$\frac{V^{n+1} - V^n}{\Delta t} - a_2 \frac{V_{xx}^{n+1} + V_{xx}^n}{2} - b_2 \frac{U^{n+1} + U^n}{2} - c_2 \frac{V^{n+1} + V^n}{2} - d_2 \frac{(U^2V)^{n+1} + (U^2V)^n}{2} \quad (11)$$
$$- e_2 \frac{(UV)^{n+1} + (UV)^n}{2} - m_2 \frac{(UV^2)^{n+1} + (UV^2)^n}{2} - n_2 = 0$$

where $U^{n+1} = U(x,t)^{n+1}$ and $V^{n+1} = V(x,t)^{n+1}$ are solutions of the equations at the $(n+1)$th time level. Here $t^{n+1} = t^n + \Delta t$ and Δt is the time step, superscripts denote the n th level $t^n = n\Delta t$.

The nonlinear terms $(U^2V)^{n+1}$, $(UV^2)^{n+1}$ and $(UV)^{n+1}$ in equation (11) are linearized by using the Rubin-Graves [33] forms:

$$(U^2V)^{n+1} = U^{n+1}U^nV^n + U^nU^{n+1}V^n + U^nU^nV^{n+1} - 2U^nU^nV^n$$

$$(UV^2)^{n+1} = U^{n+1}V^nV^n + U^nV^{n+1}V^n + U^nV^nV^{n+1} - 2U^nV^nV^n \quad (12)$$

$$(UV)^{n+1} = U^{n+1}V^n + U^nV^{n+1} - U^nV^n$$

Then we substitute (12) in (11) and the linearized model of the equation system (2) results in the following form:

$$-\frac{a_1}{2}U_{xx}^{n+1} + \beta_{m1}U^{n+1} + \beta_{m2}V^{n+1} = \frac{a_1}{2}U_{xx}^n + \beta_{m3}U^n + \beta_{m4}V^n + n_1$$

$$\quad (13)$$

$$-\frac{a_2}{2}V_{xx}^{n+1} + \beta_{m5}U^{n+1} + \beta_{m6}V^{n+1} = \frac{a_2}{2}V_{xx}^n + \beta_{m7}U^n + \beta_{m8}V^n + n_2$$

where

$$\beta_{m1} = \frac{1}{\Delta t} - \frac{b_1}{2} - d_1U^nV^n - \frac{e_1}{2}V^n - \frac{m_1}{2}(V^n)^2$$

$$\beta_{m2} = \frac{1}{\Delta t} - \frac{c_1}{2} - \frac{d_1}{2}(U^n)^2 - \frac{e_1}{2}U^n - m_1U^nV^n$$

$$\beta_{m3} = \frac{1}{\Delta t} + \frac{b1}{2} - \frac{m1}{2}(V^n)^2$$

$$\beta_{m4} = \frac{c1}{2} - \frac{d1}{2}(U^n)^2$$

$$\quad (14)$$

$$\beta_{m5} = -\frac{b_2}{2} - d_2U^nV^n - \frac{e_2}{2}V^n - \frac{m_2}{2}(V^n)^2$$

$$\beta_{m6} = \frac{1}{\Delta t} - \frac{c_2}{2} - \frac{d_2}{2}(U^n)^2 - \frac{e_2}{2}U^n - m_2U^nV^n$$

$$\beta_{m7} = \frac{b_2}{2} - \frac{m_2}{2}(V^n)^2$$

$$\beta_{m8} = \frac{1}{\Delta t} + \frac{c_2}{2} - \frac{d_2}{2}(U^n)^2.$$

We substitute the approximate solutions (8) into (13) which yields the fully-discretized equations in space.

$$\mu_{m1}\delta_{m-2}^{n+1} + \mu_{m2}\gamma_{m-2}^{n+1} + \mu_{m3}\delta_{m-1}^{n+1} + \mu_{m4}\gamma_{m-1+}^{n+1} + \mu_{m5}\delta_m^{n+1} + \mu_{m6}\gamma_m^{n+1} +$$
$$\mu_{m7}\delta_{m+1}^{n+1} + \mu_{m8}\gamma_{m+1}^{n+1} + \mu_{m9}\delta_{m+2}^{n+1} + \mu_{m10}\gamma_{m+2}^{n+1} =$$
$$\mu_{m11}\delta_{m-2}^{n} + \mu_{m12}\gamma_{m-2}^{n} + \mu_{m13}\delta_{m-1}^{n} + \mu_{m14}\gamma_{m-1}^{n} + \mu_{m15}\delta_m^{n} + \mu_{m16}\gamma_m^{n} +$$
$$\mu_{m17}\delta_{m+1}^{n} + \mu_{m18}\gamma_{m+1}^{n} + \mu_{m19}\delta_{m+2}^{n} + \mu_{m20}\gamma_{m+2}^{n} + n_1$$

$$(15)$$

$$\mu_{m21}\delta_{m-2}^{n+1} + \mu_{m22}\gamma_{m-2}^{n+1} + \mu_{m23}\delta_{m-1}^{n+1} + \mu_{m24}\gamma_{m-1}^{n+1} + \mu_{m25}\delta_m^{n+1} + \mu_{m26}\gamma_m^{n+1} +$$
$$\mu_{m27}\delta_{m+1}^{n+1} + \mu_{m28}\gamma_{m+1}^{n+1} + \mu_{m29}\delta_{m+2}^{n+1} + \mu_{m30}\gamma_{m+2}^{n+1} =$$
$$\mu_{m31}\delta_{m-2}^{n} + \mu_{m32}\gamma_{m-2}^{n} + \mu_{m33}\delta_{m-1}^{n} + \mu_{m34}\gamma_{m-1}^{n} + \mu_{m35}\delta_m^{n} + \mu_{m36}\gamma_m^{n} +$$
$$\mu_{m37}\delta_{m+1}^{n} + \mu_{m38}\gamma_{m+1}^{n} + \mu_{m39}\delta_{m+2}^{n} + \mu_{m40}\gamma_{m+2}^{n} + n_2$$

where the μ_m coefficients are:

$$\mu_{m1} = \beta_{m1}\alpha_1 - \frac{a_1}{2}\alpha_6 \qquad \mu_{m11} = \beta_{m3}\alpha_1 + \frac{a_1}{2}\alpha_6 \qquad \mu_{m21} = \beta_{m5}\alpha_1 \qquad \mu_{m31} = \beta_{m7}\alpha_1$$

$$\mu_{m2} = \beta_{m2}\alpha_1 \qquad \mu_{m12} = \beta_{m4}\alpha_1 \qquad \mu_{m22} = \beta_{m6}\alpha_1 + \frac{a_2}{2}\alpha_6 \qquad \mu_{m32} = \beta_{m8}\alpha_1 - \frac{a_2}{2}\alpha_6$$

$$\mu_{m3} = \beta_{m1}\alpha_2 - \frac{a_1}{2}\alpha_7 \qquad \mu_{m13} = \beta_{m3}\alpha_2 + \frac{a_1}{2}\alpha_7 \qquad \mu_{m23} = \beta_{m5}\alpha_2 \qquad \mu_{m33} = \beta_{m7}\alpha_2$$

$$\mu_{m4} = \beta_{m2}\alpha_2 \qquad \mu_{m14} = \beta_{m4}\alpha_2 \qquad \mu_{m24} = \beta_{m6}\alpha_2 + \frac{a_2}{2}\alpha_7 \qquad \mu_{m34} = \beta_{m8}\alpha_2 - \frac{a_2}{2}\alpha_7$$

$$\mu_{m5} = \beta_{m1}\alpha_3 - \frac{a_1}{2}\alpha_8 \qquad \mu_{m15} = \beta_{m3}\alpha_3 + \frac{a_1}{2}\alpha_8 \qquad \mu_{m25} = \beta_{m5}\alpha_3 \qquad \mu_{m35} = \beta_{m7}\alpha_3$$

$$\mu_{m6} = \beta_{m2}\alpha_3 \qquad \mu_{m16} = \beta_{m4}\alpha_3 \qquad \mu_{m26} = \beta_{m6}\alpha_3 + \frac{a_2}{2}\alpha_8 \qquad \mu_{m36} = \beta_{m8}\alpha_3 - \frac{a_2}{2}\alpha_8$$

$$\mu_{m7} = \beta_{m1}\alpha_2 - \frac{a_1}{2}\alpha_7 \qquad \mu_{m17} = \beta_{m3}\alpha_2 + \frac{a_1}{2}\alpha_7 \qquad \mu_{m27} = \beta_{m5}\alpha_2 \qquad \mu_{m37} = \beta_{m7}\alpha_2$$

$$\mu_{m8} = \beta_{m2}\alpha_2 \qquad \mu_{m18} = \beta_{m4}\alpha_2 \qquad \mu_{m28} = \beta_{m6}\alpha_2 + \frac{a_2}{2}\alpha_7 \qquad \mu_{m38} = \beta_{m8}\alpha_2 - \frac{a_2}{2}\alpha_7$$

$$\mu_{m9} = \beta_{m1}\alpha_1 - \frac{a_1}{2}\alpha_6 \qquad \mu_{m19} = \beta_{m3}\alpha_1 + \frac{a_1}{2}\alpha_6 \qquad \mu_{m29} = \beta_{m5}\alpha_1 \qquad \mu_{m39} = \beta_{m7}\alpha_1$$

$$\mu_{m10} = \beta_{m2}\alpha_1 \qquad \mu_{m20} = \beta_{m4}\alpha_1 \qquad \mu_{m30} = \beta_{m6}\alpha_1 + \frac{a_2}{2}\alpha_6 \qquad \mu_{m40} = \beta_{m8}\alpha_1 - \frac{a_2}{2}\alpha_6$$

$$(16)$$

The system (15) can be written in the following form of a ten banded matrix system:

$$A\boldsymbol{x}^{n+1} = B\boldsymbol{x}^n + F \qquad (17)$$

$$A =$$

$$
\begin{bmatrix}
\mu_{m1} & \mu_{m2} & \mu_{m3} & \mu_{m4} & \mu_{m5} & \mu_{m6} & \mu_{m7} & \mu_{m8} & \mu_{m9} & \mu_{m10} & & & & \\
\mu_{m21} & \mu_{m22} & \mu_{m23} & \mu_{m24} & \mu_{m25} & \mu_{m26} & \mu_{m27} & \mu_{m28} & \mu_{m29} & \mu_{m30} & & & & \\
 & & \mu_{m1} & \mu_{m2} & \mu_{m3} & \mu_{m4} & \mu_{m5} & \mu_{m6} & \mu_{m7} & \mu_{m8} & \mu_{m9} & \mu_{m10} & & \\
 & & \mu_{m21} & \mu_{m22} & \mu_{m23} & \mu_{m24} & \mu_{m25} & \mu_{m26} & \mu_{m27} & \mu_{m28} & \mu_{m29} & \mu_{m30} & & \\
 & & \cdots & \cdots & \cdots & \cdots & \cdots & \cdots & \cdots & \cdots & \cdots & \cdots & \cdots & \cdots \\
 & & & & \mu_{m1} & \mu_{m2} & \mu_{m3} & \mu_{m4} & \mu_{m5} & \mu_{m6} & \mu_{m7} & \mu_{m8} & \mu_{m9} & \mu_{m10} \\
 & & & & \mu_{m21} & \mu_{m22} & \mu_{m23} & \mu_{m24} & \mu_{m25} & \mu_{m26} & \mu_{m27} & \mu_{m28} & \mu_{m29} & \mu_{m30}
\end{bmatrix}
$$

$$B =$$

$$
\begin{bmatrix}
\mu_{m11} & \mu_{m12} & \mu_{m13} & \mu_{m14} & \mu_{m15} & \mu_{m16} & \mu_{m17} & \mu_{m18} & \mu_{m19} & \mu_{m20} & & & & \\
\mu_{m31} & \mu_{m32} & \mu_{m33} & \mu_{m34} & \mu_{m35} & \mu_{m36} & \mu_{m37} & \mu_{m38} & \mu_{m39} & \mu_{m40} & & & & \\
 & & \mu_{m11} & \mu_{m12} & \mu_{m13} & \mu_{m14} & \mu_{m15} & \mu_{m16} & \mu_{m17} & \mu_{m18} & \mu_{m19} & \mu_{m20} & & \\
 & & \mu_{m31} & \mu_{m32} & \mu_{m33} & \mu_{m34} & \mu_{m35} & \mu_{m36} & \mu_{m37} & \mu_{m38} & \mu_{m39} & \mu_{m40} & & \\
 & & \cdots & \cdots & \cdots & \cdots & \cdots & \cdots & \cdots & \cdots & \cdots & \cdots & \cdots & \cdots \\
 & & & & \mu_{m11} & \mu_{m12} & \mu_{m13} & \mu_{m14} & \mu_{m15} & \mu_{m16} & \mu_{m17} & \mu_{m18} & \mu_{m19} & \mu_{m20} \\
 & & & & \mu_{m31} & \mu_{m32} & \mu_{m33} & \mu_{m34} & \mu_{m35} & \mu_{m36} & \mu_{m37} & \mu_{m38} & \mu_{m39} & \mu_{m40}
\end{bmatrix}
$$

$$(18)$$

The system (17) contains $2N + 2$ equations and $2N + 10$ unknowns with the vectors x^{n+1}, x^n and F as:

$$\boldsymbol{x}^{n+1} = [\delta_{-2}^{n+1}, \gamma_{-2}^{n+1}, \delta_{-1}^{n+1}, \gamma_{-1}^{n+1}, \delta_0^{n+1}, \gamma_0^{n+1} \ldots, \delta_{N+1}^{n+1}, \gamma_{N+1}^{n+1}, \delta_{N+2}^{n+1}, \gamma_{N+2}^{n+1}]^T \tag{19}$$

$$\boldsymbol{x}^n = [\delta_{-2}^n, \gamma_{-2}^n, \delta_{-1}^n, \gamma_{-1}^n, \delta_0^n, \gamma_0^n \ldots, \delta_{N+1}^n, \gamma_{N+1}^n, \delta_{N+2}^n, \gamma_{N+2}^n]^T \tag{20}$$

$$F = [n_1, n_2, n_1, n_2, \ldots, n_1, n_2]^T \tag{21}$$

To make the above system solvable, we need additional eight constraints. On the system (17), by imposing both Dirichlet and Neumann boundary conditions helps us to eliminate parameters: δ_{-2}, $\delta_{-1}, \delta_{N+1}, \delta_{N+2}, \gamma_{-2}, \gamma_{-1}, \gamma_{N+1}, \gamma_{N+2}$. So that, resulting $(2N + 2) \times (2N + 2)$ matrix system will be solvable with Matlab program by the Gauss elimination algorithm.

In order to begin the iteration process for calculating the numerical solution, the initial parameters; $\boldsymbol{x}^0 = (\delta_{-2}^0, \gamma_{-2}^0, \delta_{-1}^0, \gamma_{-1}^0, \delta_0^0, \gamma_0^0, \ldots, \delta_{N+1}^0, \gamma_{N+1}^0, \delta_{N+2}^0, \gamma_{N+2}^0)$ must be found once by using both initial and boundary conditions. The recurrence relationship (17) gives the time evolution of vector $\boldsymbol{x}^n$. Thus the nodal values $U_N(x, t)$ and $V_N(x, t)$ can be computed via the equations (8).

3. RESULTS OF THE NUMERICAL SOLUTIONS

The aim of this section is to show the efficiency of the algorithm by studying on four different RDS and comparing the accuracy of the suggested method on the selected problems. The accuracy of the suggested method is measured with the discrete error norm for the problems which have an analytical solution:

$$L_2 = |U - U_N|_2 = \sqrt{h \sum_{j=0}^N (U_j - (U_N)_j^n)} , \tag{22}$$

$$L_\infty = |U - U_N|_\infty = \max_j |U_j - (U_N)_j^n|. \tag{23}$$

Also, the relative error is used to measure the error if there is no analytic solution of the system.

$$RE = \sqrt{\frac{\sum_{j=0}^{N} |U_j^{n+1} - U_j^n|^2}{\sum_{j=0}^{N} |U_j^{n+1}|^2}} \qquad (24)$$

The efficiency of the algorithm is exhibited by studying four different RD mechanism. For the purpose of observing the stability of the recursive system (17), the matrix stability analysis is performed and system (17) is written as in the converted matrix form as below:

$$x^{n+1} = Wx^n + Q \qquad (25)$$

Here, the iterative converted matrix is $W = A^{-1}$ and its eigenvalues λ_i are expected to be $max|\lambda_i| < 1$ to satisfy the criteria for the stability. Accordingly, eigenvalues $|\lambda_i|$ of W are computed and depicted in Figures 1-2 for the nonlinear problems; Brusselator and Schnakenberg Models.
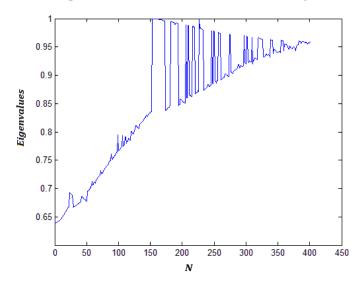

Figure 1. Eigenvalues of W obtained for Brusselator model when $N = 400$, $\Delta t = 0.01$, $t = 15$.
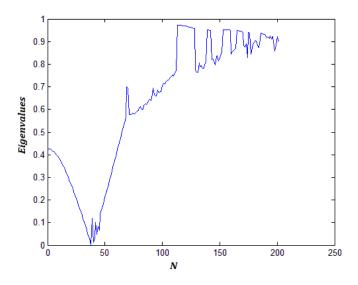

Figure 2. Eigenvalues of W obtained for Schnakenberg model when $N = 200$, $\Delta t = 5 \times 10^{-6}$, $t = 2.5$

During the run of the algorithm, we have observed that the absolute values of the eigenvalues are almost less than 1 at all time steps. Therefore the demonstrated eigenvalues in the Figs.1-2 are calculated at a specific time step. When similar treatments are performed for other test problems, it is observed that the absolute values of the eigenvalues are less than 1. In this way, the solution scheme of the recursive formula is unconditionally stable.

3.1. Linear Problem

It is stated that the terms $F(U,V)$ and $G(U,V)$ are nonlinear in the system (1). However it is not possible to calculate the error norms due to the limitations of the analytical solutions of the nonlinear system. Here, the linear problem with known analytical solutions is selected and has the form

$$\frac{\partial U}{\partial t} = d\frac{\partial^2 U}{\partial x^2} - aU + V$$

$$\frac{\partial V}{\partial t} = d\frac{\partial^2 V}{\partial x^2} - bV. \tag{26}$$

and the known analytical exact solutions are;

$$U(x,t) = \left(e^{-(a+d)t} + e^{-(b+d)t}\right)cos(x), \qquad V(x,t) = (a-b)(e^{-(b+d)t})cos(x). \tag{27}$$

The (26) system's initial conditions are induced from the analytical solution by taking $t = 0$ in the solutions of (27). Solution space is taken as $[0,\frac{\pi}{2}]$ and the set of boundary conditions which is used for eliminating the unknown parameters are:

$$U_x(0,t) = 0, \qquad U\left(\frac{\pi}{2},t\right) = 0, \qquad V_x(0,t) = 0, \qquad V\left(\frac{\pi}{2},t\right) = 0,$$

$$U_{xxx}(0,t) = 0, \qquad U_{xx}\left(\frac{\pi}{2},t\right) = 0, \qquad V_{xxx}(0,t) = 0, \qquad V_{xx}(\pi/2,t) = 0. \tag{28}$$

To analyze the dominance of reaction or diffusion, three different cases are considered. The reaction-diffusion mechanism (26) is numerically calculated with different values of parameters a, b, and d. Respectively, considered cases and parameters are;

• Case of diffusion dominated ($a = 0.1$, $b = 0.01$ and $d = 1$)

• Case of reaction dominated ($a = 2, b = 1, d = 0.001$)

• Case of reaction dominated with stiff reaction ($a = 100, b = 1, d = 0.001$)

To get numerical results, software program is run up to time level $t = 1$ for various N and Δt. The boundary and initial conditions are chosen to coincide with the PQBCM [19]. The obtained results for U and V in terms of L_2 and L_∞ norms are given in Tables 2, 3 and 4 also with comparison of the results [19] and [6] when $N = 512$ and Δt. It is observed that the accuracy of the obtained results for function V are slightly efficient than results for function U. The proposed method has a better accuracy than the ones given in Tables 2, 3 ,4 under the same conditions. In conclusion presented algorithm produces similar error norms with those of the polinomial quintic B-spline collocation [19] and Implicit integrator factor and Multi-grid solver[6].

Table 2. Error norms L_2 and L_∞ for the case of diffusion dominated when $a = 0.1$, $b = 0.01$, $d = 1$, $N = 512$

	$U(TQB)$		$V(TQB)$		$U(PQBCM)$		$V(PQBCM)$	
Δt	$L_2 \times 10^4$	$L_\infty \times 10^4$	$L_2 \times 10^6$	$L_\infty \times 10^6$	$L_2 \times 10^4$	$L_\infty \times 10^4$	$L_2 \times 10^6$	$L_\infty \times 10^6$
0.005	0.008090	0.009120	0.029344	0.033079	0.015123	0.017048	0.062416	0.070361
0.01	0.053460	0.060265	0.216594	0.244162	0.060493	0.068193	0.249667	0.281444
0.02	0.234949	0.264853	0.965627	1.088530	0.241983	0.272782	0.998702	1.125815
0.04	0.961033	1.083353	3.962253	4.466566	0.968068	1.091283	3.995334	4.503855
	$U(CN - MG$ method$)$							
0.005	0.0116							
0.01	0.0627							
0.02	0.267							
0.04	1.09							

Table 3. Error norms $\underline{L_2}$ and L_∞ for the case of reaction dominated when $a = 2$, $b = 1$, $d = 0.001$, $N = 512$

	$U(TQB)$		$V(TQB)$		$U(PQBCM)$		$V(PQBCM)$	
Δt	$L_2 \times 10^4$	$L_\infty \times 10^4$	$L_2 \times 10^5$	$L_\infty \times 10^5$	$L_2 \times 10^4$	$L_\infty \times 10^4$	$L_2 \times 10^3$	$L_\infty \times 10^3$
0.005	0.026827	0.030241	0.068087	0.076753	0.026832	0.030247	0.068124	0.076795
0.01	0.107324	0.120984	0.272462	0.307141	0.107329	0.120989	0.272499	0.307183
0.02	0.429339	0.483984	1.089996	1.228729	0.429344	0.483990	1.090033	1.228771
0.04	1.717837	1.936481	4.360663	4.915683	1.717842	1.936487	4.360700	4.915725
	$U(CN - MG$ method$)$							
0.005	0.0302							
0.01	0.121							
0.02	0.484							
0.04	1.94							

Table 4. Error norms L_2 and L_∞ for the case of diffusion dominated with stiff reaction when $a = 100$, $b = 1$, $d = 0.001$, $N = 512$

	$U(TQB)$		$V(TQB)$		$U(PQBCM)$		$V(PQBCM)$	
Δt	$L_2 \times 10^5$	$L_\infty \times 10^5$	$L_2 \times 10^3$	$L_\infty \times 10^3$	$L_2 \times 10^5$	$L_\infty \times 10^5$	$L_2 \times 10^3$	$L_\infty \times 10^3$
0.005	0.068087	0.076753	0.067406	0.075986	0.068124	0.076795	0.067443	0.076027
0.01	0.272462	0.307141	0.269738	0.304070	0.272499	0.307183	0.269774	0.304111
0.02	1.089996	1.228729	1.079096	1.216442	1.090033	1.228771	1.079133	1.216484
0.04	4.360663	4.915684	4.317057	4.866527	4.360700	4.915725	4.317093	4.866568
	$V(CN - MG$ method$)$							
0.005				0.0760				
0.01				0.304				
0.02				1.22				
0.04				4.87				

3.2. Brusselator Model

Brusselator model is mainly defined to get a kinetic model having a limit cycle. It was also shown to represents steady state, oscillatory and chaotic solutions and mentioned by Prigogine and Lefever in the study [29]. This type of RD mechanism exhibits Turing instability and large-scale studies have been conducted on this model being investigated both analytically and numerically. The general 1D reaction-diffusion equation system for this type of model is given as [3]

$$\frac{\partial U}{\partial t} = \varepsilon_1 \frac{\partial^2 U}{\partial x^2} + A + U^2 V - (B+1)U$$

$$\frac{\partial V}{\partial t} = \varepsilon_2 \frac{\partial^2 V}{\partial x^2} + BU - U^2 V \tag{29}$$

where $\varepsilon_1, \varepsilon_2$ are diffusion parameters, x is the spatial coordinate and U, V are functions of x and t representing concentrations. Initial conditions are specified as in the reference [3];

$$U(x,0) = 0.5, \qquad V(x,0) = 1 + 5x. \tag{30}$$

Following boundary conditions are considered at the end points of the problem domain:

$$U_x(x_0,t) = 0, \qquad U_x(x_N,t) = 0, \qquad V_x(x_0,t) = 0, \qquad V_x(x_N,t) = 0.$$
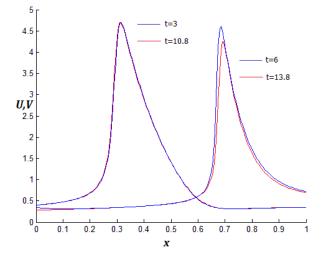$$U_{xx}(x_0,t) = 0, \qquad U_{xx}(x_N,t) = 0, \qquad V_{xx}(x_0,t) = 0 \qquad V_{xx}(x_N,t) = 0. \tag{31}$$

Figure 3: Periodic wave motion of U for Brusselator model when $N = 200, \Delta t = 0.01$
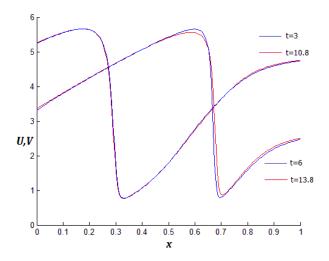

Figure 4. Periodic wave motion for V for Brusselator model when $N = 200, \Delta t = 0.01$

Suggested algorithm is performed for the equation system (29), taking the parameters as $\varepsilon_1 = \varepsilon_2 = 10^{-4}$, $A = 1, B = 3.4$, over the region $x \in [0,1]$. Computation is carried out until $t = 15$. Split points

$N = 200$, time step $\Delta t = 0.01$ are used for space and time discretization respectively. Obtained solutions are depicted in Figure 3 and Figure 4. They show changes of the density of the functions of U and V. It has been observed that both U and V wave motions exhibits periodic waves under these conditions.

Obtained density values for periodic motion are presented in Table 5. We found that the period of this wave action is about 7.8 with the proposed method, whereas the period 7.7 is found when the PQBCM [19] is implemented which is shown in the Tables 5- 6. Proposed method produces equivalent patterns with the references [9,19, 20].

Table 5. Density values of periodic motion when TQB is implemented.

Density	t	$x = 0.0$	$x = 0.2$	$x = 0.4$	$x = 0.6$	$x = 0.8$	$x = 1.0$
U	3	0.284595	0.317799	0.377380	0.604709	1.623703	0.691906
	10.8	0.344555	0.321243	0.376194	0.605486	1.715194	0.716792
	6	0.400865	0.687572	2.884364	0.549937	0.323697	0.348838
	13.8	0.398971	0.680057	2.911740	0.533798	0.322405	0.347582
V	3	3.363723	4.250910	5.066610	5.546754	1.650507	2.507119
	10.8	3.309473	4.240150	5.062313	5.651837	1.591938	2.473710
	6	5.258678	5.632343	1.073700	2.739517	4.300681	4.755329
	13.8	5.241915	5.634312	1.065232	2.769906	4.269058	4.737755

Table 6. Density values of periodic motion when PQBCM [19] is implemented.

Density	t	$x = 0.0$	$x = 0.2$	$x = 0.4$	$x = 0.6$	$x = 0.8$	$x = 1.0$
U	3	0.284657	0.317966	0.377959	0.612881	1.519483	0.648434
	10.7	0.347747	0.321168	0.376204	0.611218	1.626310	0.680742
	6	0.401741	0.706734	2.716642	0.510302	0.326204	0.352411
	13.7	0.398904	0.691408	2.769059	0.500480	0.324523	0.350579
V	3	3.363896	4.251219	5.066734	5.537413	1.732740	2.580615
	10.7	3.299664	4.233913	5.056668	5.637796	1.659946	2.534846
	6	5.257254	5.606791	1.137215	2.825295	4.355469	4.798749
	13.7	5.234725	5.613815	1.119445	2.846165	4.317357	4.774541

3.3. Schnakenberg Model

The Schnakenberg model is used to model autocatalytic chemical reaction with possible oscillatory behaviors and it is a relatively easy system for modelling the reaction-diffusion mechanism. Firstly it was put forward by Schakenberg [30] and can be stated as follows:

$$\frac{\partial U}{\partial t} = \frac{\partial^2 U}{\partial x^2} + \zeta(a - U + U^2 V)$$

$$\frac{\partial V}{\partial t} = d\frac{\partial^2 V}{\partial x^2} + \zeta(b - U^2 V) \tag{32}$$

Here, U and V represent the concentration of activator and inhibitor respectively, d is a diffusion coefficient, ζ, a and b are rate parameters of the biochemical reactions. The results of the proposed method were obtained by studying the oscillation problem in the Schnakenberg Model. Accordingly, the parameters are taken as $a = 0.126779$, $b = 0.792366$, $d = 10$ and $\zeta = 10^4$ for system (32). Graphical solutions are obtained on the interval $[-1,1]$ and the initial conditions are taken as:

$$U(x,0) = 0.919145 + 0.001 \sum_{j=1}^{25} \frac{\cos(2\pi j x)}{j} \tag{33}$$

$$V(x,0) = 0.937903 + 0.001 \sum_{j=1}^{25} \frac{cos(2\pi jx)}{j}$$

The boundary conditions are taken as:

$$U_x(x_0,t) = 0, \qquad U_x(x_N,t) = 0, \qquad V_x(x_0,t) = 0 \qquad V_x(x_N,t) = 0,$$

$$U_{xxx}(x_0,t) = 0, \qquad U_{xxx}(x_N,t) = 0, \qquad V_{xxx}(x_0,t) = 0, \qquad V_{xxx}(x_N,t) = 0. \tag{34}$$

Computations are performed until $t = 2.5$ for space/time combinations. Obtained relative errors are depicted in Table 7 together with the errors results of the PQBCM [19].

Table 7. Obtained values of relative errors for Schnakenberg model when $N = 100$ and $t = 2,5$.

Δt	Nu. of step	U	U[19]	V	V[19]
5×10^{-6}	500000	0	5.7160×10^{-14}	5.4418×10^{-17}	5.4564×10^{-14}
5×10^{-5}	50000	6.2202×10^{-17}	1.5653×10^{-10}	1.6794×10^{-16}	1.1105×10^{-10}
1×10^{-4}	25000	1.7593×10^{-16}	9.8744×10^{-10}	2.4423×10^{-16}	8.8599×10^{-10}
1.20×10^{-4}	20833	1.5668×10^{-16}	1.5055×10^{-09}	2.2996×10^{-16}	1.3790×10^{-09}
1.32×10^{-4}	18939	1.4610×10^{-16}	1.0564×10^{-01}	2.9664×10^{-16}	1.0301×10^{-01}
1×10^{-3}	2500	2.5895×10^{-14}	-	2.0341×10^{-14}	-
2×10^{-3}	1250	5.4591×10^{-09}	-	3.9448×10^{-09}	-
5×10^{-3}	500	5.4960×10^{-06}	-	4.7003×10^{-06}	-

The algorithm produces quite accurate results even when the time step is larger as observed in Table 7. Small error values are achieved even for a *Δt* as large as one with method of TQB. PQBCM needs time steps that are a factor of 200 times smaller than TQB to achieve the same accuracy. TQB method is more efficient than PQBCM method in terms of Schnakenberg Model. Graphics of Figure 5 show the oscillation movements for time increment $\Delta t = 5 \times 10^{-5}$ and split points of $N = 100$ and $N = 200$ respectively. The functions U and V make 9 oscillations when $N = 100$ and $N = 200$ as depicted in Figure 5. This result and the references [1] and [2] show that a finer mesh is necessary for accurate solutions.
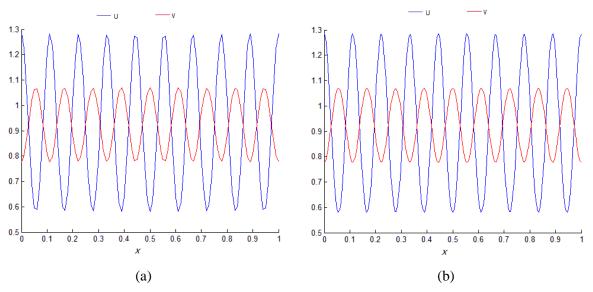

(a)   (b)

Figure 5. The oscillation waves of U and V for Schnakenberg model, when (a) $N = 100$, $t = 2.5$ (b) $N = 200$, $t = 2.5$

3.4. Gray-Scott Model

The Gray-Scott model is a widely known type of reaction-diffusion system which models some spatial patterns to be formed by several chemical species in nature. Formerly it was presented by Gray and Scott [31] and defined:

$$\frac{\partial U}{\partial t} = \varepsilon_1 \frac{\partial^2 U}{\partial x^2} - U^2 V + f(1 - U),$$

$$\frac{\partial V}{\partial t} = \varepsilon_2 \frac{\partial^2 V}{\partial x^2} + U^2 V - kV \tag{35}$$

The proposed method is implemented on the repeating spot patterns exhibited by the Gray-Scott model. The parameters are selected in accordance with the reference [32] for the system (35)

$$\varepsilon_1 = 1, \quad \varepsilon_2 = 0.01, \quad a = 9, \quad b = 0.4, \quad f = \varepsilon_2 a, \quad k = \varepsilon_2^{1/3} b \tag{36}$$

Also the initial conditions of the system (35) are selected as:

$$U(x,0) = 1 - \frac{1}{2} sin^{100}\left(\pi \frac{(x-L)}{2L}\right), \quad V(x,0) = \frac{1}{4} sin^{100}(\pi \frac{(x-L)}{2L}) \tag{37}$$

Space discretization $N = 400$ and time discretization $\Delta t = 0.2$ are taken and solutions are computed in $L \in [-50,50]$. Dirichlet and additional Neuman boundary conditions

$$U(x_0, t) = 1, \quad U(x_N, t) = 1, \quad V(x_0, t) = 0, \quad V(x_N, t) = 0,$$

$$U_x(x_0, t) = 0, \quad U_x(x_N, t) = 0, \quad V_x(x_0, t) = 0, \quad V_x(x_N, t) = 0. \tag{38}$$

are applied. The self replicating waves are obtained when the program is run until to the time level $t = 1000$. Under these initial conditions, primarily two pulses are created and separated from each other, then each pulse at the edges are being split into two again to form four pulses, as shown in Figure 6 until time $t = 1000$, as time evolved. These self-replicating process goes on to cover the spatial domain. The replicating process of U and V functions due to time and space are presented in Figures 6(a)(b)(c).

The intensity changes of functions U and V due to time and space are presented respectively in Figure 7 and Figure 8. These spatial patterns, which are kind of growing Turing patterns, initially starting with two waves of splitting movement, seem to cover the whole domain with branching over time. The obtained patterns are similar and compatible with [19, 32]
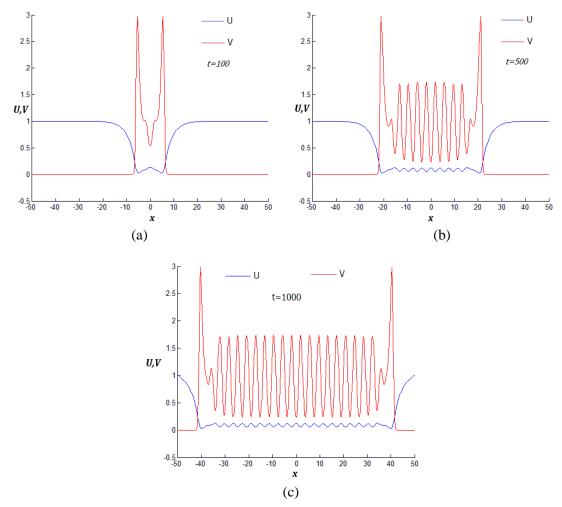
(a)

(b)

(c)

Figure 6. The replicating process of spot patterns for Gray-Scott model when (a) $t = 100$, (b) $t = 500$ and (c) $t = 1000$
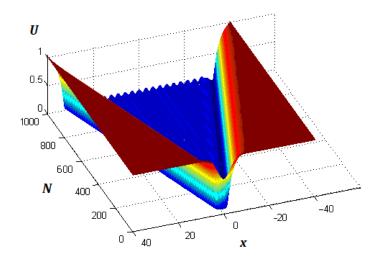

Figure 7. Graphical illustration of U for Gray-Scott model, when $N = 200, \Delta t = 0.01$
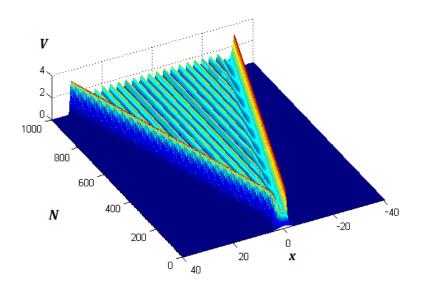
Figure 8. Graphical illustration of V for Gray-Scott model, when $N = 200, \Delta t = 0.01$

4. CONCLUSION

The continuum problem represented by the reaction-diffusion system is transformed into a discrete problem with a finite number of variables such that suggested method replaces the continuous problem with an algebraic system. The proposed method is well suited for approximating accurate solutions of the reaction-diffusion systems for pattern formation. For the validation of the suggested algorithm, approximate solutions of linear and nonlinear RD systems are shown on the models of certain chemical and biological problems. Firstly the method is conducted for getting numerical solution of the linear reaction diffusion system, for which the analytical solution exists. $L2$ norms of the computational solutions are quite satisfactory and are similar with the reported work of the polynomial quintic B-spline collocation method and better than the Crank-Nicolson-multigrid method when the same parameters are used. Nonlinear reaction-diffusion systems known as the Brusselator model, Schnakenberg model and Gray-Scott models are also simulated suitably. Solutions of the nonlinear problems, which have no analytical solutions in general, are given graphically. All of model solutions are represented fairly and can be compared with the equivalent graphs given in the studies [1-3, 19, 20, 32]. Also approximate solution of the Schnakenberg model with proposed method produced better error values. Use of the trigonometric quintic B-spline having continuity of order four allows us to have an approximate functions in order of four. Therefore, differential equations in order of four can be solved numerically by using the trigonometric B-spline functions to have solutions of continuity in order of four.

Computational cost of the algorithm depends on the gauss elimination method while solving the matrix system. As a computational cost, number of the basic operations can be calculated as $O((2N + 1)^2 \times \frac{t}{\Delta t})$. Since the resulting matrix is band matrix, it is solved by the Gauss elimination method, so the storage capacity is reduced and speed of the algorithm is accelerated. Therefore the method is easily implemented for such reaction-diffusion models. Consequently, the TQB collocation method produces fairly acceptable results for numerical investigation of RD systems. Thus, it is also recommended for finding solutions of other partial differential equations and fractional partial differential equations.

ACKNOWLEDGMENT

CONFLICT OF INTEREST

The authors stated that there are no conflicts of interest regarding the publication of this article.

AUTHORSHIP CONTRIBUTIONS

The algorithm design of the non linear problem was suggested by Idiris Dağ. The numerical solutions of the problem, algorithm construction and coding as well as the writing of the article in English, were carried out by Aysun Tok Onarcan. Nihat Adar provided support during the coding phase and writing of the article.

REFERENCES

[1] Ruuth SJ. Implicit-explicit methods for reaction-diffusion problems in pattern formation. J Math Bio 1995; 34: 148-176.

[2] Madzvamuse A, Wathen AJ, Maini PK. A moving grid finite element method applied to a biological pattern generator. J Comp Phys 2003; 190: 478-500.

[3] Zegeling PA, Kok HP. Adaptive moving mesh computations for reaction-diffusion systems. J Comp App Math 2004; 168: 519-528.

[4] Ropp DL, Shadid JN, Ober CC. Studies of the accuracy of time integration methods for reaction-diffusion equations. J Comp Phys 2004; 194(2): 544-574.

[5] Ropp DL, Shadid JN. Stability of operator splitting methods for systems with indefinite operators: reaction-diffusion systems. J Comp Phys 2005; 203(2): 449-466.

[6] Chou CS, Zhang Y, Zhao R, Nie Q. Numerical Methods for Stiff Reaction-Diffusion Systems. Discrete and Continuous Dynamical Systems-Series B 2007;7: 515-525.

[7] Yadav OP, Jiwari R. A finite element approach for analysis and computational modelling of coupled reaction diffusion models. Numerical Methods for Partial Differential Equations 2019; 35 (2): 830-850.

[8] Mittal RC, Rohila R. Numerical Simulation of Reaction-Diffusion Systems by Modified Cubic B-spline Differential Quadrature Method. Chaos, Solitons and Fractals 2016; 92 (1): 1339-1351.

[9] Jiwari R, Singh S, Kumar A. Numerical simulation to capture the pattern formation of coupled reaction-diffusion models. Chaos, Solitons and Fractals 2017; 103: 422-439.

[10] Jiwari R, Gerisch A. A local radial basis function differential quadrature semidiscretisation technique for the simulation of time-dependent reaction-diffusion problems. Eng Comp 2016; 38 (6): 2666-2691.

[11] Schoenberg IJ. On Trigonometric Spline Interpolation. J Math Mech 1964;13: 795-826.

[12] Hamid NNA, Majid AA, Ismail AIM. Cubic Trigonometric B-spline Applied to Linear Two-Point Boundary Value Problems of Order Two. World Academy of Science, Engineering and Technology 2010; 47: 478-803.

[13] Gupta Y, Kumar MA Computer Based Numerical Method for Singular Boundary Value Problems. Int J Comp App 2011;1: 0975-8887.

[14] Zin SM, Abbas M, Majid AA, Ismail AIM. A New Trigonometric Spline Approach to Numerical Solution of Generalized Nonlinear Klien-Gordon Equation. PLoS one, 2014;9(5): e95774.

[15] Abbas M, Majid AA, Ismail AIM, Rashid A. Numerical Method Using Cubic Trigonometric B-Spline Technique for Nonclassical Diffusion Problems. Abstract and Applied Analysis, 2014; Article ID 849682.

[16] Yağmurlu NM, Karakaş AS. Numerical solutions of the equal width equation by trigonometric cubic B-spline collocation method based on Rubin–Graves type linearization. Num Meth Part Diff Eqs, 2020; 36(5): 1170-1183.

[17] Nikolis A. Numerical Solutions of Ordinary Differential Equations with Quadratic Trigonometric Splines. App Maths E-Notes 2004;4: 142-149.

[18] Nikolis A, Seimenis I. Solving Dynamical Systems with Cubic Trigonometric Splines. App Maths E-notes, 2005; 5: 116-123.

[19] Sahin A. Numerical solutions of the reaction-diffusion equations with B-spline finite element method. PhD, Eskişehir Osmangazi University, Eskişehir, Turkey, 2009.

[20] Ersoy O, Dag I. Numerical Solutions of the Reaction Diffusion System by Using Exponential Cubic B-spline Collocation Algorithms. Open Phys 2015; 13: 414-427.

[21] Onarcan AT, Adar N, Dag I. Trigonometric cubic B-spline collocation algorithm for numerical solutions of reaction–diffusion equation systems. Comp App Math 2018; 37: 6848–6869.

[22] Tok-Onarcan A, Adar N, Dag I. Wave simulations of Gray-Scott reaction-diffusion system. Math Meth in the App Sci 2019; 19: 5566–5581.

[23] Kaur N, Joshi V. Numerical solution to the Gray-Scott Reaction-Diffusion equation using Hyperbolic B-spline. J Phys: Conference Series 2022: 2267.

[24] Hepson ÖE, Yiğit G, Allahviranloo T. Numerical simulations of reaction–diffusion systems in biological and chemical mechanisms with quartic-trigonometric B-splines. Comp App Math 2021; 40(4): 1-23.

[25] Hepson ÖE, Numerical solutions of the Gardner equation via trigonometric quintic B-spline collocation method, Sakarya Üniversitesi Fen Bilimleri Enstitüsü Dergisi 2018; 22 (6): 1576–1584.

[26] Chandrasekharan Nair L, Awasthi A. Quintic trigonometric spline based numerical scheme for nonlinear modified Burgers' equation, Num Meth for Part Diff Eq 2019; 35(3): 1269–1289.

[27] Khater MMA, Nisar KS, Mohamed MS. Numerical investigation for the fractional nonlinear space-time telegraph equation via the trigonometric Quintic B-spline scheme. Math Meth in App Sci 2021; 44(6); 4598–4606.

[28] Alam MP, Kumar D, Khan A. Trigonometric quintic B-spline collocation method for singularly perturbed turning point boundary value problems. Int J Comp Math 2021;98(5): 1029–1048.

[29]   Prigogine I, Lefever R. Symmetry Breaking Instabilities in Dissipative Systems. J Chem Phys 1968; 48:1695-1700.

[30]   Schnakenberg J. Simple Chemical Reaction Systems with Limit Cycle Behavior. J Theo Bio 1979; 81: 389-400.

[31]   Gray P, Scott SK. Autocatalytic Reactions in The Isothermal, Continuous Stirred Tank Reactor: Oscillations and Instabilities in the system A+2B 3B, B C. Chem Eng Sci, 1984;39: 1087-1097.

[32]   Craster RV, Sassi R. Spectral Algorithms for Reaction-Diffusion Equations. Technical Report. Note del Polo 2006: No:99.

[33]   Rubin SG, Graves Jr RA. A cubic spline approximation for problems in fluid mechanics. Technical Report, Nasa, Washington, 1975.